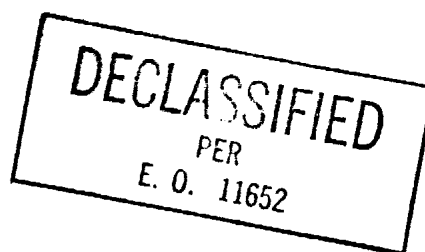


**NASA TECHNICAL  
MEMORANDUM**



UB  
NASA TM X-1566

UB  
NASA TM X-1566



**HEAT-TRANSFER EFFECTS  
OF SURFACE PROTUBERANCES  
ON THE X-15 AIRPLANE**

*by Joe D. Watts and Frank V. Olinger*

*Flight Research Center  
Edwards, Calif.*

HEAT-TRANSFER EFFECTS OF SURFACE PROTUBERANCES  
ON THE X-15 AIRPLANE

By Joe D. Watts and Frank V. Olinger

Flight Research Center  
Edwards, Calif.

GROUP 4  
Downgraded at 3 year intervals;  
declassified after 12 years

CLASSIFIED DOCUMENT-TITLE UNCLASSIFIED

This material contains information affecting the national defense of the United States within the meaning of the espionage laws, Title 18, U.S.C., Secs. 793 and 794, the transmission or revelation of which in any manner to an unauthorized person is prohibited by law.

NOTICE

This document should not be returned after it has satisfied your requirements. It may be disposed of in accordance with your local security regulations or the appropriate provisions of the Industrial Security Manual for Safe-Guarding Classified Information.

NATIONAL AERONAUTICS AND SPACE ADMINISTRATION

# HEAT-TRANSFER EFFECTS OF SURFACE PROTUBERANCES ON THE X-15 AIRPLANE\*

By Joe D. Watts and Frank V. Olinger  
Flight Research Center

## SUMMARY

The heat-transfer effects of flow separation forced by two types of surface protuberances on the fuselage of the X-15 airplane were measured in flight at Mach numbers near 5 and local Reynolds numbers of approximately  $5 \times 10^7$ . The two protuberance configurations were a 0.20-inch (0.51-centimeter) forward-and-aft-facing step and a sine wave of 0.20-inch- (0.51-centimeter-) amplitude at a right angle to the stream direction. Heat-transfer coefficients were calculated from measured skin temperatures across the protuberances and normalized to measured smooth-panel data. The variation of the heat-transfer coefficient across the protuberances ranged from 0.09 to 2.23 times the smooth-surface value. Flight data were compared with wind-tunnel data measured in turbulent flow.

## INTRODUCTION

The adverse heating effects of surface protuberances such as panel-edge discontinuities, skin buckles, cavities, and corrugations can be of great importance in the design of hypersonic vehicles. Consequently, the local aerodynamic-heating effects of separated flow forced by surface protuberances have been the subject of many wind-tunnel investigations in recent years. A wide variety of surface-protuberance configurations has been investigated but most of the data has been obtained in laminar flow at low stagnation temperatures and low Reynolds numbers.

One of the primary purposes of flight tests on the X-15 airplane was to extend the data beyond the conditions in wind-tunnel tests such as those discussed in references 1 and 2. This paper presents the results of flight heat-transfer measurements on two protuberance configurations: a forward-and-aft-facing step at a Mach number of 4.6 and a Reynolds number of  $6 \times 10^7$ , and a sine-wave corrugation at a right angle to the stream direction at a Mach number of 5.2 and a Reynolds number of  $4 \times 10^7$ . The ratio of boundary-layer thickness to protuberance height  $\frac{\delta}{y}$  was 14 on the step test and 18 on the wave test, in contrast to most wind-tunnel data, which are in the  $\frac{\delta}{y}$  range of 0.25 to 2.00.

---

\*Title, unclassified.

## SYMBOLS

The units used for physical quantities in this paper are given both in U. S. Customary Units and the International System of Units (SI). Factors relating the two systems are presented in the appendix.

$c_{p,w}$	specific heat of panel material, 0.117 British thermal units per pound (mass)-degrees Rankine (489 joules per kilogram-degrees Kelvin)
$F$	radiation geometry factor, 1.0
$H$	altitude, feet (meters)
$h$	heat-transfer coefficient, British thermal units per foot <sup>2</sup> -second-degrees Rankine (joules per meter <sup>2</sup> -second-degrees Kelvin)
$k$	thermal conductivity, British thermal units per foot-second-degrees Rankine (joules per meter-second-degrees Kelvin)
$M$	Mach number
$N_{Re,l}$	local Reynolds number, $\frac{\rho V_l s}{\mu}$
$p$	absolute pressure, pounds per foot <sup>2</sup> (newtons per meter <sup>2</sup> )
$s$	flow length measured from nose of fuselage, feet (meters)
$T$	temperature, degrees Rankine (degrees Kelvin)
$T_R$	recovery temperature, degrees Rankine (degrees Kelvin)
$t_w$	material thickness, feet (meters)
$V$	velocity, feet per second (meters per second)
$x$	distance along test panel, inches (centimeters)
$y$	protuberance height, inches (centimeters)
$\alpha$	angle of attack, degrees

$\delta$	boundary-layer thickness, inches (centimeters)
$\epsilon$	emissivity of panel-material surface, 0.76
$\mu$	dynamic viscosity of air, pounds (mass) per foot-second (newton-seconds per meter <sup>2</sup> )
$\rho$	density of air, pounds (mass) per foot <sup>3</sup> (kilograms per meter <sup>3</sup> )
$\rho_w$	density of skin material, 515 pounds (mass) per foot <sup>3</sup> (8250 kilograms per meter <sup>3</sup> )
$\sigma$	Stefan-Boltzmann constant, $4.78 \times 10^{-13}$ British thermal units per foot <sup>2</sup> -second-degrees Rankine <sup>4</sup> ( $5.67 \times 10^{-8}$ watts per meter <sup>2</sup> -degrees Kelvin <sup>4</sup> )
$\tau$	time, seconds
Subscripts:	
$l$	local conditions
$o$	reference panel conditions (smooth surface)
$w$	wall or skin
$\infty$	free stream

## DESCRIPTION OF TESTS AND INSTRUMENTATION

The X-15 airplane, shown in figure 1, was launched from a B-52 carrier aircraft at about 45,000 feet (13,700 meters) altitude, climbed under full power to the desired altitude, and attained level flight at reduced throttle with speed brakes extended to stabilize the velocity. The data for this experiment were taken during the period of quasi-steady flight just prior to fuel depletion. The final portion of the flight was a glide back to a landing at Edwards Air Force Base, Calif.

The Inconel X test panels used in the experiment were on the lower surface of the fuselage, 28 feet (8.5 meters) aft of the nose. The panels were exposed to aerodynamic heating throughout the entire flight. Figure 2 shows the location of the protuberance panel and the smooth reference panel on the airplane. The forward edge of the panels was approximately 12 inches (30 centimeters) aft of the liquid-oxygen tank. The protuberance geometry, instrumentation, and dimensions for the step configuration and the wave configuration are shown in figures 3 and 4, respectively. The smooth reference panel was instrumented with one central thermocouple. The thermocouples were 30-gage chromel-alumel wires, spot-welded to the inner surface of the panel. The recording system sampled the thermocouple data 2.5 times per second.

Airplane velocity and altitude were obtained from a radar tracking system. Free-stream temperature, pressure, and wind corrections for velocity were obtained from balloon soundings. Airplane attitudes were obtained from the X-15 inertial guidance system and flow-direction sensor. Time histories of pertinent parameters starting from launch are shown in figure 5 for flight A (step configuration) and in figure 6 for flight B (wave configuration). The data time intervals used in this report are shown in figures 5 and 6 by the cross hatched areas. The data listings in tables I through IV have their data time referenced to the data time interval used.

## DATA REDUCTION

The heat-transfer coefficients presented in this report were determined by using the following equation:

$$h = \frac{\rho_w c_{p,w} t_w \left( \frac{dT_w}{d\tau} \right)}{(T_R - T_w)} + \frac{\sigma \epsilon F T_w^4}{(T_R - T_w)} - \frac{k t_w \left( \frac{d^2 T_w}{dx^2} \right)}{(T_R - T_w)} \quad (144) \quad (1)$$

where the numerator of the first term is the heat stored in a unit area of the surface, the numerator of the second term is the heat reradiated to the atmosphere, and the numerator of the last term is the heat gained or lost by conduction in the skin. The factor 144 in the conduction term is needed to maintain unit consistency. The properties of the skin are known, the wall temperature and rate of change of wall temperature are measured, and the recovery temperature is calculated by using a recovery factor of 0.89. Heat-transfer coefficients were calculated using equation (1) at data time 2.8 seconds.

The first two terms of equation (1) were calculated with a digital computer, using a least-squares-curve fit to determine  $\frac{dT_w}{d\tau}$ . The second derivative in the correction factor was obtained by plotting the streamwise temperature distribution, fairing a smooth curve through the points, and graphically determining the slope at each point on the curve to obtain the first derivative. The first derivative was then plotted as a function of streamwise distance, a smooth curve faired through the points, and the slope graphically determined at each point along the curve to obtain the second derivative. Finally, the second derivative was plotted against streamwise distance, and a smooth curve was faired through the points. Values for the second derivative used in the correction factor were taken from the final smooth curve. Figures 7(a), (b), and (c) show the temperature distribution and the first and second derivatives for a representative portion of the sine-wave test panel. For purposes of the conduction correction on the step configuration only, the distance along the surface of the step was used instead of the streamwise distance. Thermocouples 11a, 11b, 11c, 20a, 20b, and 20c on the vertical faces of the step were used to correct the heat-transfer data for conduction at thermocouples 11, 12, 20, and 21 but were not included in the heat-transfer distribution.

The following assumptions were made in the analysis of the data:

1. The smooth-surface recovery temperature  $T_R$  was assumed to apply in the vicinity of the protuberances.

2. Two-dimensional flow was assumed.
3. Internal radiation loss was neglected. Heat loss due to internal radiation was minimized by gold-plating the internal surface of the panels.
4. Lateral temperature gradients on the panels were negligible.
5. The streamwise temperature distribution along the smooth reference panel was constant, represented by the single reference thermocouple in the center of the panel. (Flight experience indicates that a negligible streamwise temperature variation would occur over a panel of this size.)
6. The local flow conditions were essentially the same as free-stream conditions for the test-panel location on the airplane. (A large amount of unpublished data obtained in this area indicates that this is a valid assumption.)

The estimated accuracy of the temperature data was  $\pm 13$  Rankine degrees ( $\pm 7.2$  Kelvin degrees), and the overall accuracy of the heat-transfer coefficients (before conduction correction) was estimated to be  $\pm 10$  percent. The conduction correction varied from 0 to 40 percent, based on the approximate method used in determining the second derivative. The maximum heat loss due to radiation to the atmosphere (second term of equation (1)) was 13.5 percent of the convective heating rate.

Boundary-layer thicknesses were computed by using the method of reference 3 together with turbulent boundary-layer parameters obtained from reference 4, assuming a one-seventh power velocity-distribution law. No attempt was made to account for the effect of the large surface temperature gradient between the liquid-oxygen tank (approximately  $160^\circ \text{R}$ ) and the test panels (approximately  $1000^\circ \text{R}$ ).

## DISCUSSION OF RESULTS

Pertinent flight parameters for the 0.20-inch (0.51-centimeter) forward-and-aft-facing step configuration are presented in table I. Temperature time histories of the thermocouple positions for the corresponding time interval are included in table II. The temperature distribution at the time heat-transfer data were reduced is shown in figure 8. The distribution of the heat-transfer ratio  $\frac{h}{h_0}$  is shown in figure 9. The peak heat-transfer ratio ahead of the protuberance was 2.23, and the peak behind the protuberance was 1.44. The lowest value of the ratio was 0.09 at the aft edge of the step. The figure shows the significant correction that had to be made to the heat-transfer data for conduction error as a result of the high-temperature gradients along the panel. It is apparent from both figures 8 and 9 that the aerodynamic heating in the vicinity of the step is affected by the step more than eight step heights upstream and downstream.

Table III contains the flight parameters for the 0.20-inch (0.51-centimeter) sine-wave corrugation and table IV presents the temperature time histories for the thermocouple positions. Figure 10 shows the temperature distribution at the time the heat-transfer data were reduced. The distribution of the heat-transfer ratio across the panel is shown in figure 11. The values of the heat-transfer ratio ranged from 0.34 to 2.03 and, as with the step configuration, a significant conduction correction was necessary.

It is interesting to note that when the heat-flux distributions across both the step and the wave configurations were integrated to determine the net heat flux into the panels at the one point in time, the value was nearly the same for the protuberances as for the smooth panel.

A comparison of flight and wind-tunnel heat-transfer-ratio distribution on a step protuberance is shown in figure 12. The ratio of boundary-layer thickness to protuberance height for the flight data is considerably larger than the ratio for wind-tunnel data. Although the levels vary considerably, the trends of the data are similar. One exception is that the first peak in the wind-tunnel data just ahead of the step is seen only as a slight change of slope in the flight data.

Figure 13 shows a comparison of flight and wind-tunnel data for a sinusoidal wave train. Good agreement was obtained for the all-turbulent flight data and the turbulent portion of the wind-tunnel data, even though there was a large difference in the ratio of boundary-layer thickness to protuberance height.

The only available method for calculating the peak heating on a wave train, that of Jaeck (ref. 5), was used and the results were compared with the peak value in the flight data. The Jaeck method underpredicted the peak value by approximately 35 percent. It is believed that the empirical nature of the method is the reason for its inadequacy for  $\frac{\delta}{y}$  values greater than 1.

#### CONCLUDING REMARKS

Heat-transfer effects of separated flow were investigated in flight tests of two protuberance configurations on the X-15 airplane. The 0.20-inch (0.51-centimeter) forward-and-aft-facing step and the 0.20-inch- (0.51-centimeter-) amplitude sine-wave oriented at a right angle to the stream direction resulted in a local heat-transfer variation of 0.09 to 2.23 and 0.34 to 2.03 times the smooth surface value, respectively.

The net heat flux into the test panels was essentially the same as on the smooth reference panel, even though there was a large variation of heat-transfer across the panels.

Flight Research Center,  
National Aeronautics and Space Administration,  
Edwards, Calif., December 14, 1967,  
126-13-03-01-24.



## APPENDIX

### CONVERSION OF U. S. CUSTOMARY UNITS TO SI UNITS

Conversion factors for the units used in this report are given in the following table:

Physical quantity	U. S. Customary Unit	Conversion factor (*)	SI Unit
Heat-transfer coefficient	Btu/ft <sup>2</sup> -sec-°R	$2.042 \times 10^4$	J/m <sup>2</sup> -sec-°K
Specific heat	Btu/lbm-°R	$4.18 \times 10^3$	J/kg-°K
Length	ft	0.3048	m
	in.	2.54	cm
Temperature	°R	0.556	°K
Velocity	ft/sec	0.3048	m/sec
Density	lbm/ft <sup>3</sup>	16.02	kg/m <sup>3</sup>

\*Multiply value given in U. S. Customary Unit by conversion factor to obtain equivalent value in SI Unit.

Prefixes to indicate multiples of units are:

Prefix	Multiple
centi (c)	$10^{-2}$
hecto (h)	$10^2$
kilo (k)	$10^3$

## REFERENCES

1. Burbank, Paige B.; Newlander, Robert A.; and Collins, Ida K.: Heat-Transfer and Pressure Measurements on a Flat-Plate Surface and Heat-Transfer Measurements on Attached Protuberances in a Supersonic Turbulent Boundary Layer at Mach Numbers of 2.65, 3.51, and 4.44. NASA TN D-1372, 1962.
2. Bertram, M. H.; Weinstein, L. M.; Cary, A. M., Jr.; and Arrington, J. P.: Heat Transfer to Wavy Wall in Hypersonic Flow. AIAA J., vol. 5, no. 10, Oct. 1967, pp. 1760-1767.
3. Reshotko, Eli; and Tucker, Maurice: Approximate Calculation of the Compressible Turbulent Boundary Layer With Heat Transfer and Arbitrary Pressure Gradient. NACA TN 4154, 1957.
4. Persh, Jerome; and Lee, Roland: Tabulation of Compressible Turbulent Boundary Layer Parameters. NAVORD Rep. 4282 (Aeroballistic Res. Rep. 337), U. S. Naval Ordnance Lab., White Oak, Md., May 1, 1956.
5. Jaeck, C. L.: Analysis of Pressure and Heat Transfer Tests on Surface Roughness Elements With Laminar and Turbulent Boundary Layers. NASA CR-537, 1966.

TABLE I. – STEP-PANEL FLIGHT CONDITIONS

[Flight A]

Data time, sec	H		V		M <sup>a</sup>	$\alpha$ , deg	P <sub>∞</sub>		T <sub>∞</sub>		N <sub>Re, <math>\ell</math></sub> <sup>a</sup>	T <sub>R</sub> <sup>a</sup>	
	ft	m	ft/sec	m/sec			lb/ft <sup>2</sup>	hN/m <sup>2</sup>	°R	°K		°R	°K
0.4	69,245	21,106	4443	1354	4.61	1.62	99.7	47.7	387	215	$6.01 \times 10^7$	1811	1007
1.6	69,436	21,164	4457	1358	4.62	1.98	98.8	47.3	387	215	6.07	1815	1009
2.8 <sup>b</sup>	69,507	21,186	4467	1362	4.63	1.44	98.4	47.1	387	215	6.04	1820	1012
4.0	69,587	21,210	4474	1364	4.64	2.16	98.0	46.9	387	215	6.02	1824	1014
5.2	69,493	21,181	4482	1366	4.64	1.53	98.5	47.2	387	215	5.99	1828	1016
6.4	69,440	21,165	4490	1369	4.65	1.53	98.7	47.2	387	215	6.01	1833	1019

<sup>a</sup>Calculated.<sup>b</sup>Time at which data were reduced.

TABLE II. – STEP-PANEL TEMPERATURES  
[Flight A]

Data time, sec	Thermocouple																	
	1		2		3		4		5		6		7		8		9	
	°R	°K	°R	°K	°R	°K	°R	°K	°R	°K	°R	°K	°R	°K	°R	°K	°R	°K
0	822	457	858	477	869	483	916	509	948	527	953	530	979	544	974	541	1004	558
0.4	827	459	858	477	885	492	927	515	948	527	953	530	994	553	989	550	1009	561
0.8	827	459	864	480	880	489	932	518	963	535	968	538	994	553	994	553	1020	567
1.2	832	463	874	486	891	495	932	518	953	530	974	542	1004	558	994	553	1020	567
1.6	843	469	874	486	896	498	942	524	979	544	979	544	1009	561	1009	561	1030	573
2.0	848	471	880	489	901	501	953	530	984	547	989	550	1020	567	1015	564	1045	581
2.4	848	471	891	495	911	507	953	530	989	550	994	553	1020	567	1030	573	1050	584
2.8	858	477	896	498	916	509	968	538	999	555	1004	558	1035	575	1040	578	1050	584
3.2	858	477	896	498	916	509	974	542	1004	558	1015	564	1040	578	1035	575	1071	595
3.6	869	483	906	504	927	515	974	542	1030	573	1015	564	1050	584	1045	581	1071	595
4.0	874	486	916	509	932	518	978	544	1020	567	1015	564	1050	584	1056	587	1076	598
4.4	880	489	916	509	942	524	984	547	1020	567	1025	570	1056	587	1056	587	1081	601
4.8	885	492	927	515	948	527	994	553	1025	570	1035	575	1066	593	1061	590	1091	607
5.2	885	492	927	515	953	530	994	553	1030	573	1020	567	1071	595	1071	595	1091	607
5.6	885	492	927	515	953	530	994	553	1030	573	1020	567	1071	595	1071	595	1091	607

Data time, sec	Thermocouple <sup>a</sup>																	
	11b		11c		12		13		14		15		16		17		18	
	°R	°K	°R	°K	°R	°K	°R	°K	°R	°K	°R	°K	°R	°K	°R	°K	°R	°K
0	1122	624	1116	620	963	535	948	527	932	518	911	507	906	504	896	498	874	486
0.4	1122	624	1126	626	974	541	958	533	932	518	916	509	911	507	906	504	880	489
0.8	1126	626	1131	629	979	544	958	533	942	524	922	513	922	513	911	507	896	498
1.2	1137	632	1131	629	989	550	968	538	948	527	930	517	927	515	916	509	896	498
1.6	1137	632	1137	632	994	552	978	544	958	516	937	521	932	518	927	515	906	504
2.0	1142	635	1147	638	1004	558	978	544	968	538	948	527	937	521	927	515	911	507
2.4	1142	635	1147	638	1009	561	989	550	968	538	948	527	942	524	932	518	916	509
2.8	1147	638	1152	641	1015	564	994	553	974	542	958	533	953	530	942	524	927	515
3.2	1152	641	1157	643	1020	567	999	555	984	547	963	535	953	530	942	524	927	515
3.6	1152	641	1162	646	1030	573	1004	558	989	550	968	538	963	535	948	527	927	515
4.0	1157	643	1162	646	1030	573	1015	564	994	553	974	542	968	538	958	533	937	521
4.4	1162	646	1167	649	1030	573	1020	567	999	555	978	544	968	538	963	535	948	527
4.8	1162	646	1177	654	1045	581	1025	570	1004	558	984	547	978	544	968	538	948	527
5.2	1172	652	1177	654	1056	587	1030	573	1009	561	989	550	984	547	974	542	958	533
5.6	1172	652	1177	654	1056	587	1040	578	1015	564	989	550	989	550	979	544	958	533

<sup>a</sup>Thermocouple 19 inoperative.

TABLE II. - STEP-PANEL TEMPERATURES - Concluded

Data time, sec	Thermocouple <sup>a</sup>																							
	20c		21		22		23		24		25		26		27		28		29		30		32	
	°R	°K	°R	°K	°R	°K	°R	°K	°R	°K	°R	°K	°R	°K	°R	°K	°R	°K	°R	°K	°R	°K	°R	°K
0	758	421	671	373	711	395	774	430	838	466	864	480	874	486	896	498	822	457	891	495	864	480	864	480
0.4	763	424	671	373	716	398	780	434	848	471	869	466	885	492	901	501	827	460	895	498	874	486	869	483
0.8	763	424	680	378	721	401	780	434	848	471	874	486	891	495	906	504	832	463	901	501	880	489	880	489
1.2	769	428	680	378	727	404	785	436	853	474	880	489	896	498	911	507	843	469	906	504	885	492	880	489
1.6	774	430	685	381	727	404	795	442	858	477	885	492	901	501	916	509	848	471	916	509	891	495	891	495
2.0	774	430	691	384	732	407	801	445	864	480	891	495	906	504	927	515	848	471	916	509	901	501	896	498
2.4	780	434	696	387	737	410	801	445	869	483	891	495	911	507	927	515	858	477	937	521	901	501	901	501
2.8	780	434	696	387	742	413	801	445	874	486	901	501	911	507	932	518	864	480	932	518	911	507	901	501
3.2	790	439	696	387	742	413	822	457	880	489	906	504	922	513	942	524	869	483	932	518	911	507	911	507
3.6	795	442	701	390	748	416	822	457	885	492	911	507	927	515	942	524	874	486	942	524	916	509	911	507
4.0	795	442	701	390	758	421	822	457	891	495	916	507	932	518	948	527	880	489	948	527	927	515	916	509
4.4	801	445	706	393	758	421	827	460	896	498	916	509	937	521	948	527	885	492	948	527	927	515	927	515
4.8	801	445	716	398	758	421	832	463	896	498	922	513	937	521	958	533	885	492	948	527	927	515	927	515
5.2	806	448	716	398	763	424	832	463	901	501	927	515	948	527	958	533	901	501	958	533	937	521	932	518
5.6	811	451	721	401	769	428	832	463	906	504	937	521	948	527	968	538	896	498	963	535	942	524	937	520

<sup>a</sup>Thermocouple 31 inoperative.TABLE III. - WAVE-PANEL FLIGHT CONDITIONS  
[Flight B]

Data time, sec	H		V		M <sup>a</sup>	$\alpha$ , deg	P <sub>∞</sub>		T <sub>∞</sub>		N <sub>Re, l</sub> <sup>a</sup>	T <sub>R</sub> <sup>a</sup>	
	ft	m	ft/sec	m/sec			lb/ft <sup>2</sup>	hN/m <sup>2</sup>	°R	°K		°R	°K
0.4	80,233	24,455	5135	1565	5.20	3.22	61.2	29.3	405	225	4.08 × 10 <sup>7</sup>	2243	1247
1.6	80,276	24,468	5151	1570	5.22	3.10	61.1	29.3	405	225	4.07	2256	1254
2.8 <sup>b</sup>	80,368	24,496	5170	1576	5.24	2.70	60.8	29.1	405	225	4.03	2271	1263
4.0	80,668	24,588	5192	1583	5.26	2.31	60.0	28.7	406	226	4.01	2287	1272
5.2	80,904	24,660	5216	1590	5.28	2.07	59.4	28.4	406	226	4.03	2303	1280
6.4	80,928	24,667	5239	1597	5.30	1.85	59.3	28.4	406	226	4.02	2316	1288

<sup>a</sup>Calculated.<sup>b</sup>Time at which data were reduced.

TABLE IV. -- WAVE-PANEL TEMPERATURES  
[Flight B]

Data time, sec	Thermocouple <sup>a</sup>													
	1		2		3		4		6		7		8	
	°R	°K	°R	°K	°R	°K	°R	°K	°R	°K	°R	°K	°R	°K
0	1076	598	1099	611	1101	612	1084	603	1038	577	984	547	981	545
0.4	1076	598	1099	611	1106	615	1099	611	1040	578	984	547	992	552
0.8	1086	604	1119	622	1111	618	1099	611	1042	579	994	553	987	549
1.2	1091	607	1109	617	1111	618	1104	614	1053	585	994	553	996	554
1.6	1096	609	1114	619	1122	624	1114	619	1059	589	1004	558	992	552
2.0	1101	612	1129	628	1124	625	1109	617	1048	583	1009	561	1002	557
2.4	1106	615	1130	628	1126	626	1129	628	1068	594	1009	561	1007	560
2.8	1106	615	1124	625	1131	629	1124	625	1074	597	1015	564	1012	563
3.2	1116	620	1134	631	1131	629	1124	625	1074	597	1020	567	1012	563
3.6	1116	620	1145	637	1142	635	1129	628	1079	600	1025	570	1023	569
4.0	1116	620	1134	631	1142	635	1140	634	1084	603	1030	573	1023	569
4.4	1122	624	1145	635	1147	635	1140	634	1074	597	1030	573	1023	569
4.8	1122	624	1150	639	1147	638	1140	634	1084	603	1035	575	1033	574
5.2	1122	624	1150	639	1152	641	1145	637	1099	611	1040	578	1043	580
5.6	1126	626	1150	639	1152	641	1155	642	1089	605	1040	578	1028	572

<sup>a</sup>Thermocouples 5 and 9 inoperative.

Data time, sec	Thermocouple													
	15		16		17		18		19		20		21	
	°R	°K	°R	°K	°R	°K	°R	°K	°R	°K	°R	°K	°R	°K
0	864	480	904	503	895	498	940	523	937	521	971	540	1009	561
0.4	869	483	914	508	901	501	930	517	937	521	981	545	1009	561
0.8	869	483	912	507	906	504	935	520	937	521	984	547	1015	564
1.2	874	486	909	505	906	504	945	525	948	527	987	549	1020	567
1.6	874	486	920	512	911	507	935	520	948	527	992	552	1020	567
2.0	885	492	930	517	916	509	951	529	948	527	997	554	1025	570
2.4	885	492	925	514	916	509	956	532	958	533	1000	556	1030	573
2.8	891	495	935	520	922	513	956	532	963	535	1002	557	1030	573
3.2	895	498	935	520	932	518	971	540	968	538	1012	563	1035	575
3.6	901	501	935	520	932	518	976	543	974	542	1023	569	1045	581
4.0	901	501	951	529	932	518	971	540	979	544	1033	574	1045	581
4.4	911	507	951	529	937	521	966	537	979	544	1028	572	1050	584
4.8	911	507	951	529	942	524	981	545	979	544	1028	572	1056	587
5.2	911	507	951	529	948	527	981	545	989	550	1043	580	1056	587
5.6	911	507	951	529	948	527	981	545	989	550	1043	580	1056	587

Data time, sec	Thermocouple																							
	27		28		29		30		31		32		33		34		35		36		37			
	°R	°K	°R	°K	°R	°K	°R	°K	°R	°K	°R	°K	°R	°K	°R	°K	°R	°K	°R	°K	°R	°K		
0	1207	671	1245	692	1247	693	1265	703	1237	688	1270	706	1217	677	1215	676	1147	638	1134	631	1081	601	601	
0.4	1212	674	1245	692	1247	693	1280	712	1247	693	1265	703	1227	682	1224	681	1152	641	1140	634	1081	601		
0.8	1212	674	1250	695	1257	699	1275	709	1252	696	1280	712	1227	682	1224	681	1157	643	1145	637	1086	604		
1.2	1221	679	1265	703	1262	702	1280	712	1252	696	1280	712	1232	685	1235	687	1167	649	1145	637	1096	609		
1.6	1227	682	1260	701	1267	704	1290	717	1257	699	1285	714	1237	688	1235	687	1172	652	1150	639	1096	609		
2.0	1232	685	1275	709	1272	707	1295	720	1267	704	1295	714	1247	693	1240	689	1177	654	1155	642	1106	615		
2.4	1237	688	1285	714	1277	710	1310	728	1272	707	1295	720	1252	696	1255	698	1177	654	1170	651	1111	618		
2.8	1242	691	1280	712	1287	716	1315	731	1277	710	1295	720	1254	697	1255	698	1182	657	1170	651	1111	618		
3.2	1242	691	1275	709	1282	713	1310	728	1277	710	1305	726	1257	699	1250	695	1187	660	1175	653	1111	618		
3.6	1247	693	1285	714	1292	718	1310	728	1282	713	1315	731	1262	702	1245	692	1192	663	1175	653	1122	624		
4.0	1252	696	1285	714	1292	718	1325	737	1287	716	1305	726	1267	704	1260	701	1192	663	1185	659	1126	626		
4.4	1252	696	1285	714	1292	718	1320	734	1287	716	1315	731	1270	706	1260	701	1202	668	1180	656	1131	629		
4.8	1257	699	1295	720	1297	721	1320	734	1292	718	1320	734	1272	707	1265	703	1197	666	1185	659	1131	629		
5.2	1262	702	1298	722	1297	721	1330	739	1292	718	1330	739	1272	707	1270	706	1212	674	1195	664	1142	635		
5.6	1262	702	1300	723	1302	724	1335	742	1297	721	1320	734	1282	713	1280	712	1212	674	1205	670	1142	635		

Data time, sec		Thermocouple																							
		38		39		40		41		42		43		44		45		46		47		48			
		°R	°K	°R	°K	°R	°K	°R	°K	°R	°K	°R	°K	°R	°K	°R	°K	°R	°K	°R	°K	°R	°K		
0		1063	591	989	550	971	540	937	521	935	520	911	507	930	517	911	507	935	520	927	515	961	534		
0.4		1063	591	990	550	980	545	940	523	925	514	916	509	935	520	911	507	925	514	932	518	961	534		
0.8		1068	594	1005	559	992	552	942	524	945	525	916	509	925	514	922	513	935	520	937	521	966	537		
1.2		1079	600	1004	558	987	549	953	530	940	523	927	515	940	523	922	513	937	521	937	521	968	538		
1.6		1074	597	1009	561	997	554	953	530	945	525	932	518	940	523	927	515	940	523	948	527	971	540		
2.0		1084	603	1015	564	1002	557	958	533	951	529	932	518	940	523	932	518	945	525	948	527	981	545		
2.4		1084	603	1020	567	1007	560	963	535	951	529	937	521	956	532	932	518	945	525	953	530	987	549		
2.8		1089	605	1030	573	1007	560	968	538	951	529	942	524	961	534	942	524	945	525	958	533	981	545		
3.2		1094	608	1035	575	1012	563	968	538	966	537	942	524	945	525	942	524	961	534	963	535	987	549		
3.6		1109	617	1035	575	1012	563	972	540	956	532	953	530	956	532	942	524	961	534	963	535	992	552		
4.0		1099	611	1040	578	1028	572	978	544	966	537	953	530	971	540	948	527	961	534	963	535	992	552		
4.4		1109	617	1040	578	1028	572	984	547	976	543	958	533	971	540	953	530	976	543	968	538	987	549		
4.8		1114	619	1045	581	1028	572	989	550	987	549	958	533	971	540	953	530	976	543	974	542	997	554		
5.2		1129	628	1050	584	1033	574	989	550	992	552	963	535	971	540	958	533	966	537	976	543	1012	563		
5.6		1119	622	1056	587	1043	580	994	553	981	545	968	538	976	543	960	534	971	540	978	544	1015	564		

TABLE IV. -- WAVE-PANEL TEMPERATURES - Concluded

Data time, sec	Thermocouple															
	49		50		51		52		53		54		55		56	
	°R	°K	°R	°K	°R	°K	°R	°K	°R	°K	°R	°K	°R	°K	°R	°K
0	942	524	981	545	984	547	1028	572	1040	578	1085	603	1081	601	1140	634
0.4	953	530	990	550	989	550	1028	572	1045	579	1085	605	1088	605	1135	631
0.8	953	530	997	554	989	550	1043	580	1045	581	1094	608	1091	607	1155	642
1.2	955	531	997	554	994	553	1043	580	1050	584	1094	608	1096	609	1155	642
1.6	958	533	1007	560	999	555	1043	580	1056	587	1109	617	1099	611	1150	639
2.0	964	536	1007	560	1004	558	1053	585	1061	590	1099	611	1101	612	1165	648
2.4	974	542	1018	566	1009	561	1059	589	1065	592	1114	619	1111	618	1160	645
2.8	978	544	1023	569	1009	561	1048	583	1071	595	1119	622	1116	620	1170	651
3.2	984	547	1023	569	1015	564	1068	594	1065	592	1104	614	1120	623	1180	656
3.6	984	547	1023	569	1020	567	1078	599	1076	598	1119	622	1126	626	1185	659
4.0	984	547	1033	574	1025	570	1063	591	1086	604	1134	631	1131	629	1175	653
4.4	988	549	1033	574	1027	571	1074	597	1086	604	1134	631	1131	629	1190	662
4.8	992	552	1048	583	1030	573	1084	603	1091	607	1140	634	1142	635	1195	664
5.2	994	553	1043	580	1032	574	1084	603	1091	607	1140	634	1142	635	1200	667
5.6	996	554	1053	585	1035	575	1079	600	1096	609	1150	639	1152	641	1205	670

Data time, sec	Thermocouple <sup>a</sup>															
	60		62		63		64		66		68		70		71	
	°R	°K	°R	°K	°R	°K	°R	°K	°R	°K	°R	°K	°R	°K	°R	°K
0	1240	689	1265	703	1227	682	1230	684	1195	664	1119	622	1043	580	989	550
0.4	1255	698	1255	698	1232	685	1235	687	1215	676	1140	634	1048	583	994	553
0.8	1255	692	1275	709	1242	691	1240	689	1205	670	1134	631	1053	585	999	555
1.2	1245	698	1285	714	1247	693	1260	701	1215	676	1145	637	1053	585	1009	561
1.6	1260	701	1275	709	1252	696	1255	698	1205	670	1145	637	1059	589	1009	561
2.0	1265	703	1290	717	1257	699	1263	702	1219	678	1150	639	1066	593	1015	564
2.4	1270	706	1290	717	1257	699	1270	706	1219	678	1160	645	1074	597	1020	567
2.8	1265	703	1290	717	1267	704	1280	712	1230	684	1160	645	1079	600	1020	567
3.2	1277	710	1300	723	1267	704	1275	709	1235	687	1160	645	1079	600	1020	567
3.6	1290	717	1302	724	1272	707	1275	709	1235	687	1170	651	1084	603	1030	573
4.0	1285	714	1305	726	1272	707	1290	717	1235	687	1175	653	1084	603	1030	573
4.4	1285	714	1310	728	1277	710	1285	714	1245	692	1170	651	1099	611	1035	575
4.8	1290	717	1320	734	1282	713	1290	717	1250	695	1180	656	1099	611	1040	578
5.2	1305	726	1325	737	1287	716	1295	720	1250	695	1185	659	1094	608	1040	578
5.6	1295	720	1315	731	1292	718	1310	728	1245	692	1185	659	1109	617	1040	578

<sup>a</sup>Thermocouples 61, 65, 67, and 69 inoperative.



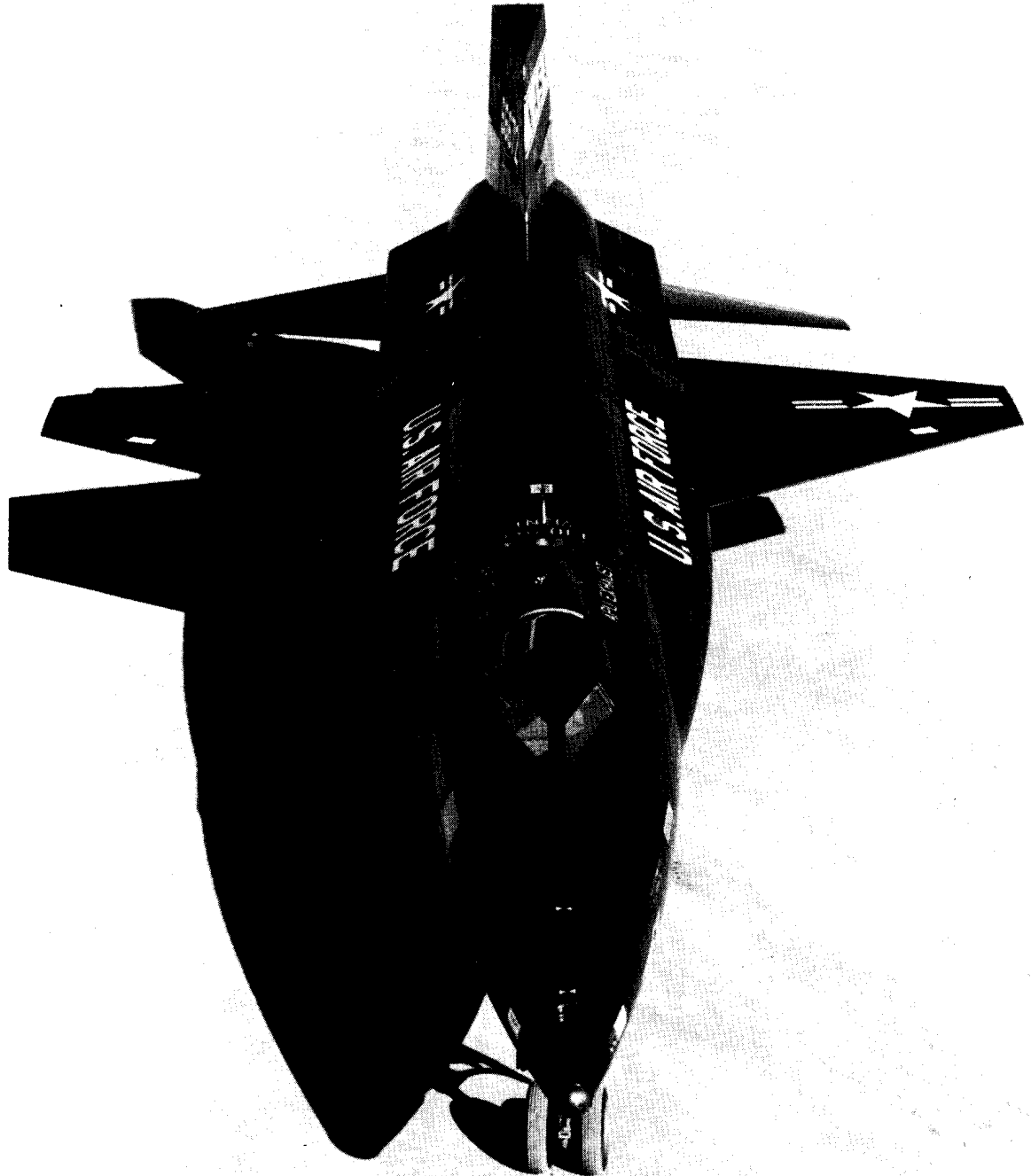


Figure 1. - X-15 airplane.

E-7903

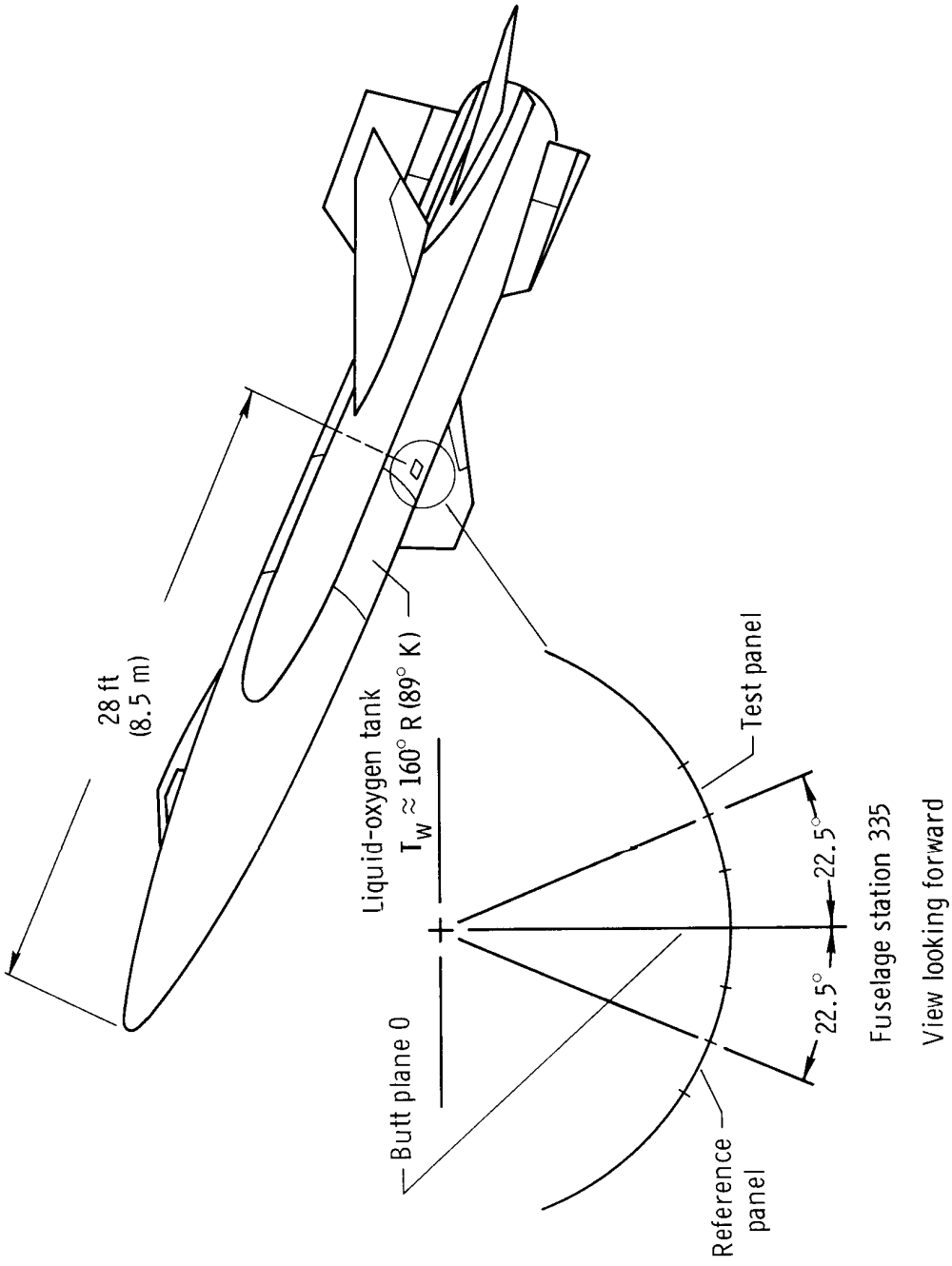
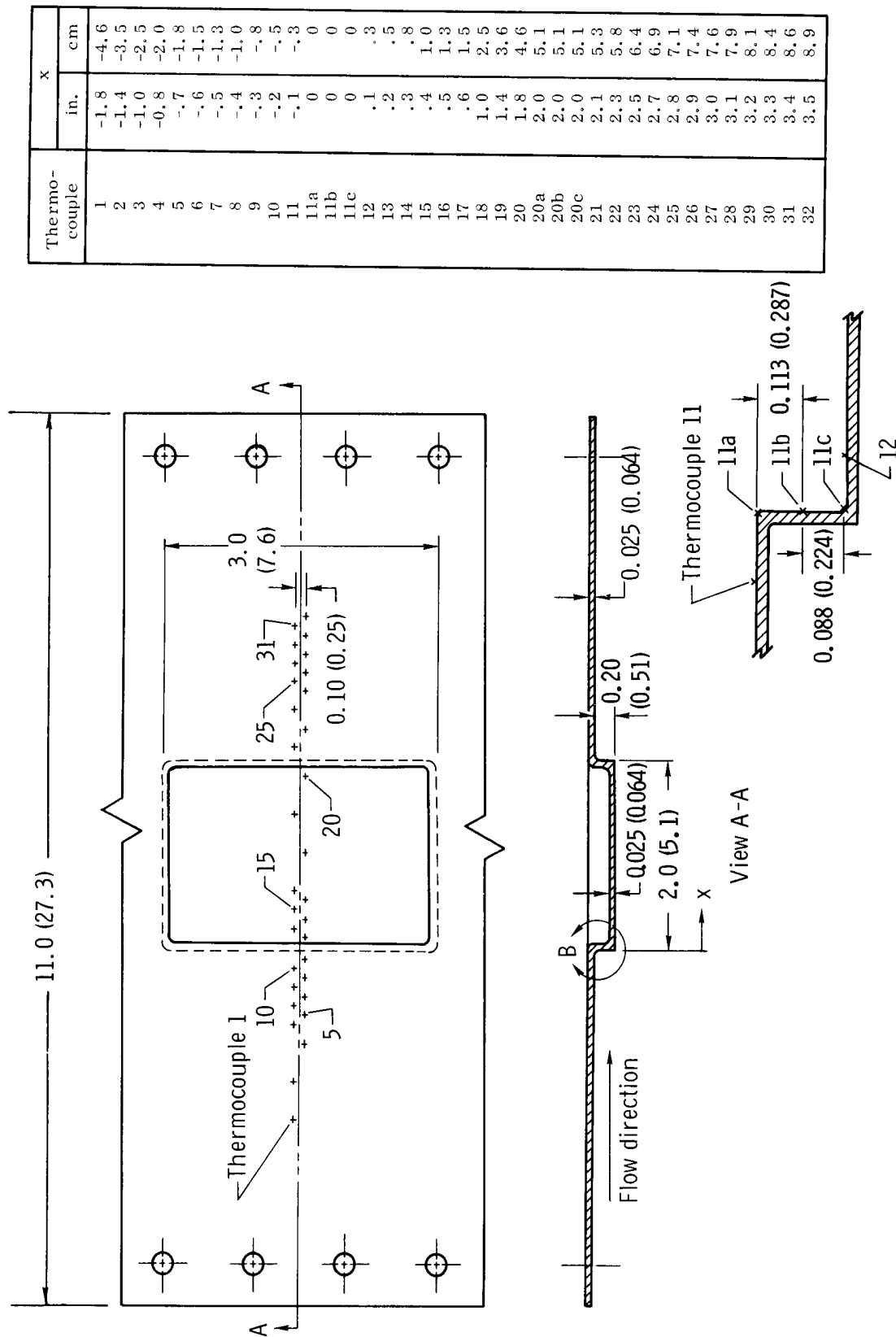


Figure 2. – Location of test and reference panels.



Thermo- couple	x	
	in.	cm
1	-1.8	-4.6
2	-1.4	-3.5
3	-1.0	-2.5
4	-0.8	-2.0
5	-0.7	-1.8
6	-0.6	-1.5
7	-0.5	-1.3
8	-0.4	-1.0
9	-0.3	-0.8
10	-0.2	-0.5
11	-0.1	-0.3
11a	0	0
11b	0	0
11c	0	0
12	.1	.3
13	.2	.5
14	.3	.8
15	.4	1.0
16	.5	1.3
17	.6	1.5
18	1.0	2.5
19	1.4	3.6
20	1.8	4.6
20a	2.0	5.1
20b	2.0	5.1
20c	2.0	5.1
21	2.1	5.3
22	2.3	5.8
23	2.5	6.4
24	2.7	6.9
25	2.8	7.1
26	2.9	7.4
27	3.0	7.6
28	3.1	7.9
29	3.2	8.1
30	3.3	8.4
31	3.4	8.6
32	3.5	8.9

Detail B  
(typical for thermocouples 20a, 20b, 20c)

Figure 3. – Step configuration. All dimensions in inches (centimeters).

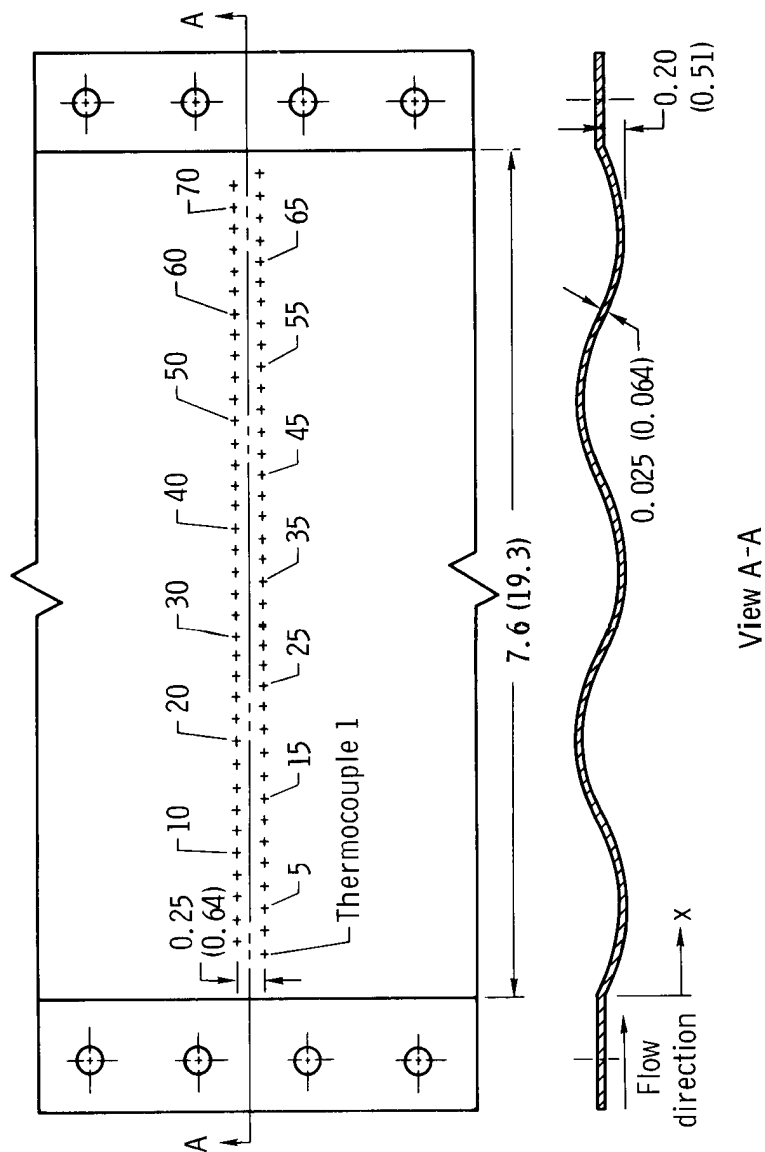


Figure 4.— Sine-wave configuration. All dimensions in inches (centimeters).

Thermo- couple	x	
	in.	cm.
1	0.3	0.8
2	.4	1.0
3	.5	1.3
4	.6	1.5
5	.7	1.8
6	.8	2.0
7	.9	2.3
8	1.0	2.5
9	1.1	2.8
10	1.2	3.0
11	1.3	3.3
12	1.4	3.6
13	1.5	3.8
14	1.6	4.1
15	1.7	4.3
16	1.8	4.6
17	1.9	4.8
18	2.0	5.1
19	2.1	5.3
20	2.2	5.6
21	2.3	5.8
22	2.4	6.1
23	2.5	6.4
24	2.6	6.6
25	2.7	6.9
26	2.8	7.1
27	2.9	7.4
28	3.0	7.6
29	3.1	7.9
30	3.2	8.1
31	3.3	8.4
32	3.4	8.6
33	3.5	8.9
34	3.6	9.1
35	3.7	9.4
36	3.8	9.6
37	3.9	9.9
38	4.0	10.2
39	4.1	10.4
40	4.2	10.7
41	4.3	10.9
42	4.4	11.2
43	4.5	11.4
44	4.6	11.7
45	4.7	11.9
46	4.8	12.2
47	4.9	12.4
48	5.0	12.7
49	5.1	12.9
50	5.2	13.2
51	5.3	13.5
52	5.4	13.7
53	5.5	14.0
54	5.6	14.2
55	5.7	14.5
56	5.8	14.7
57	5.9	15.0
58	6.0	15.2
59	6.1	15.5
60	6.2	15.7
61	6.3	16.0
62	6.4	16.3
63	6.5	16.5
64	6.6	16.8
65	6.7	17.0
66	6.8	17.3
67	6.9	17.5
68	7.0	17.8
69	7.1	18.0
70	7.2	18.3
71	7.3	18.5
72	7.4	18.8
73	7.5	19.1

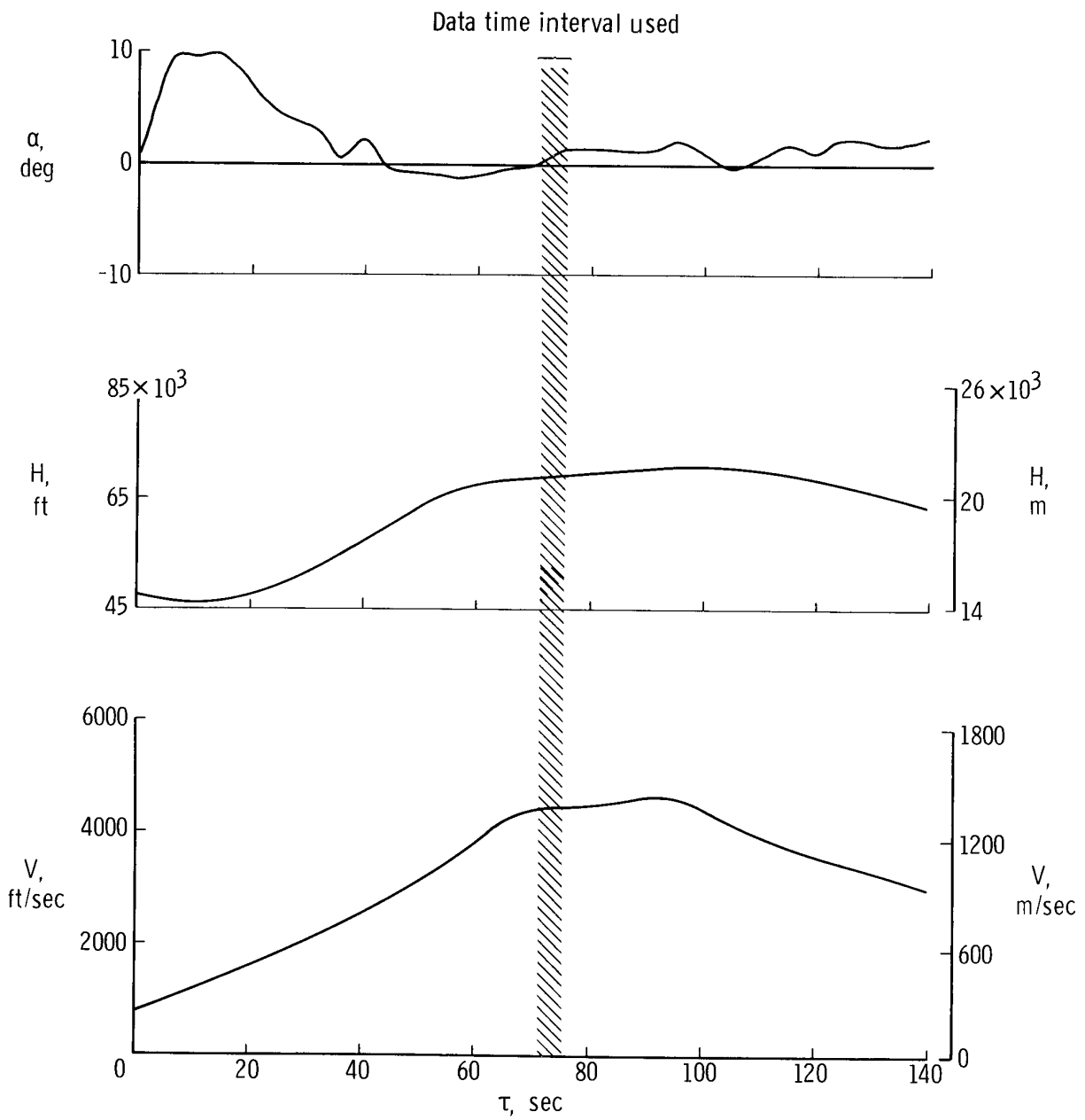


Figure 5. — Flight conditions for step configuration, flight A.

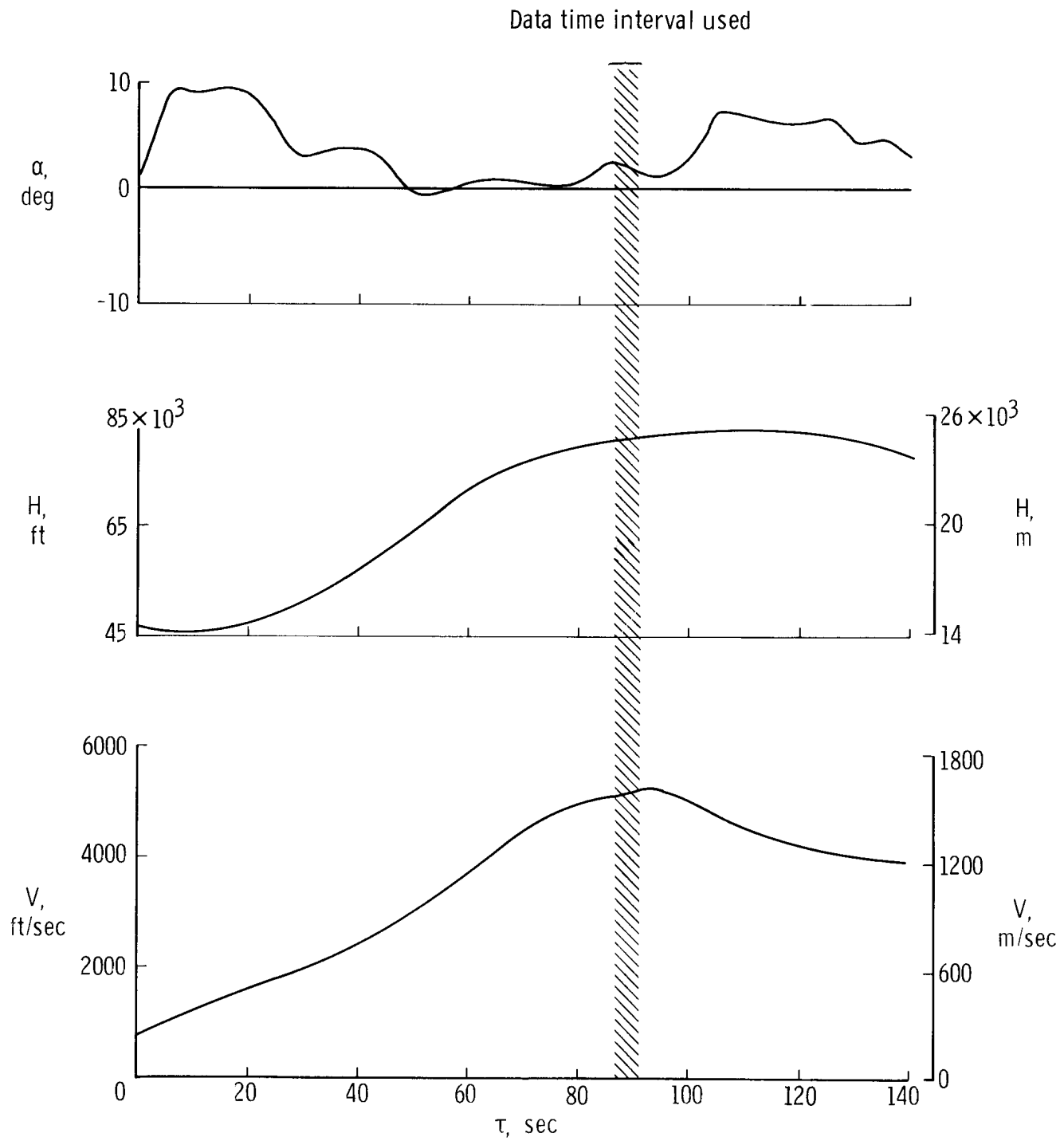


Figure 6.— Flight conditions for wave configuration, flight B.

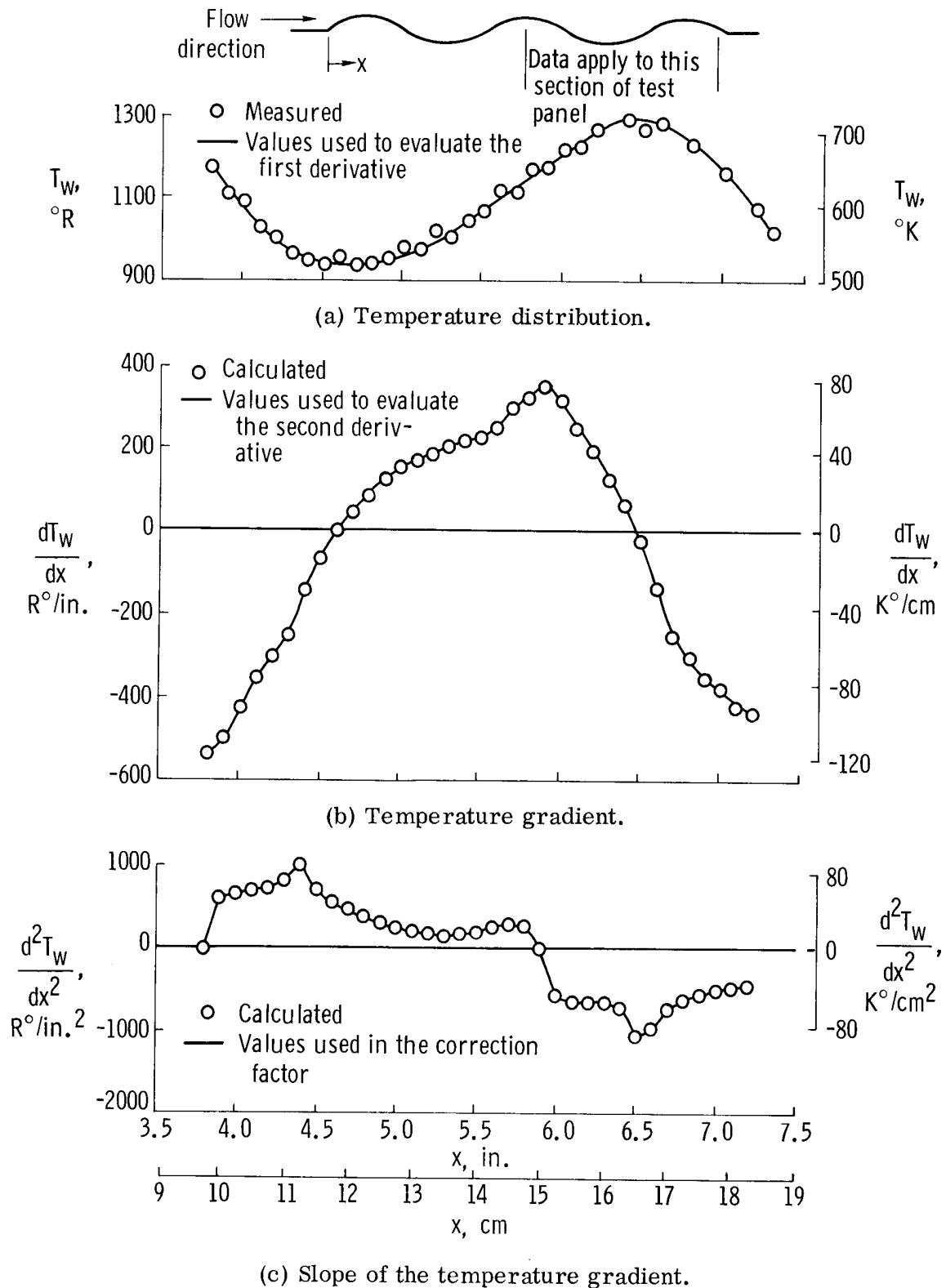


Figure 7.— Temperature distribution, temperature gradient, and slope of the temperature gradient for a sample portion of the wave configuration.

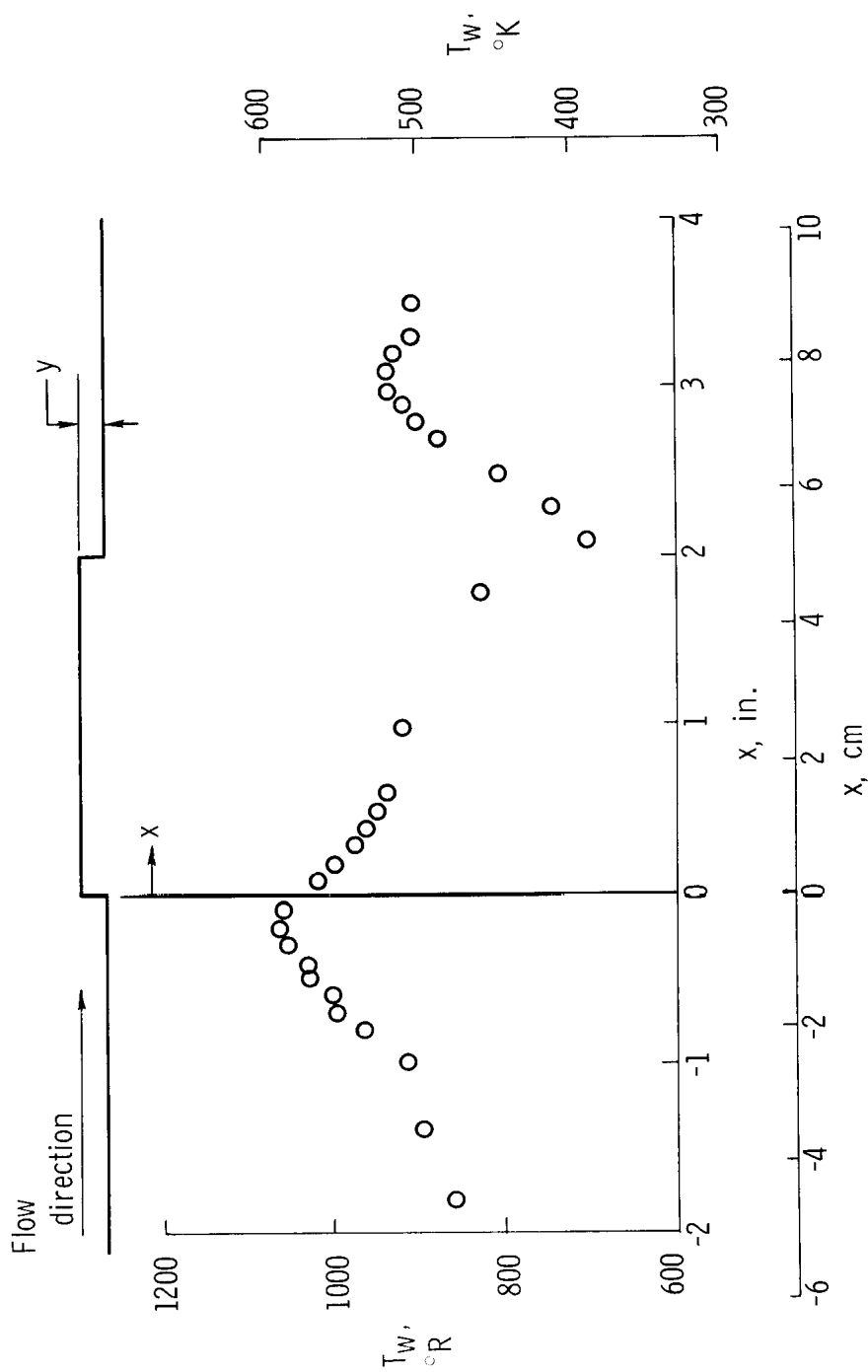
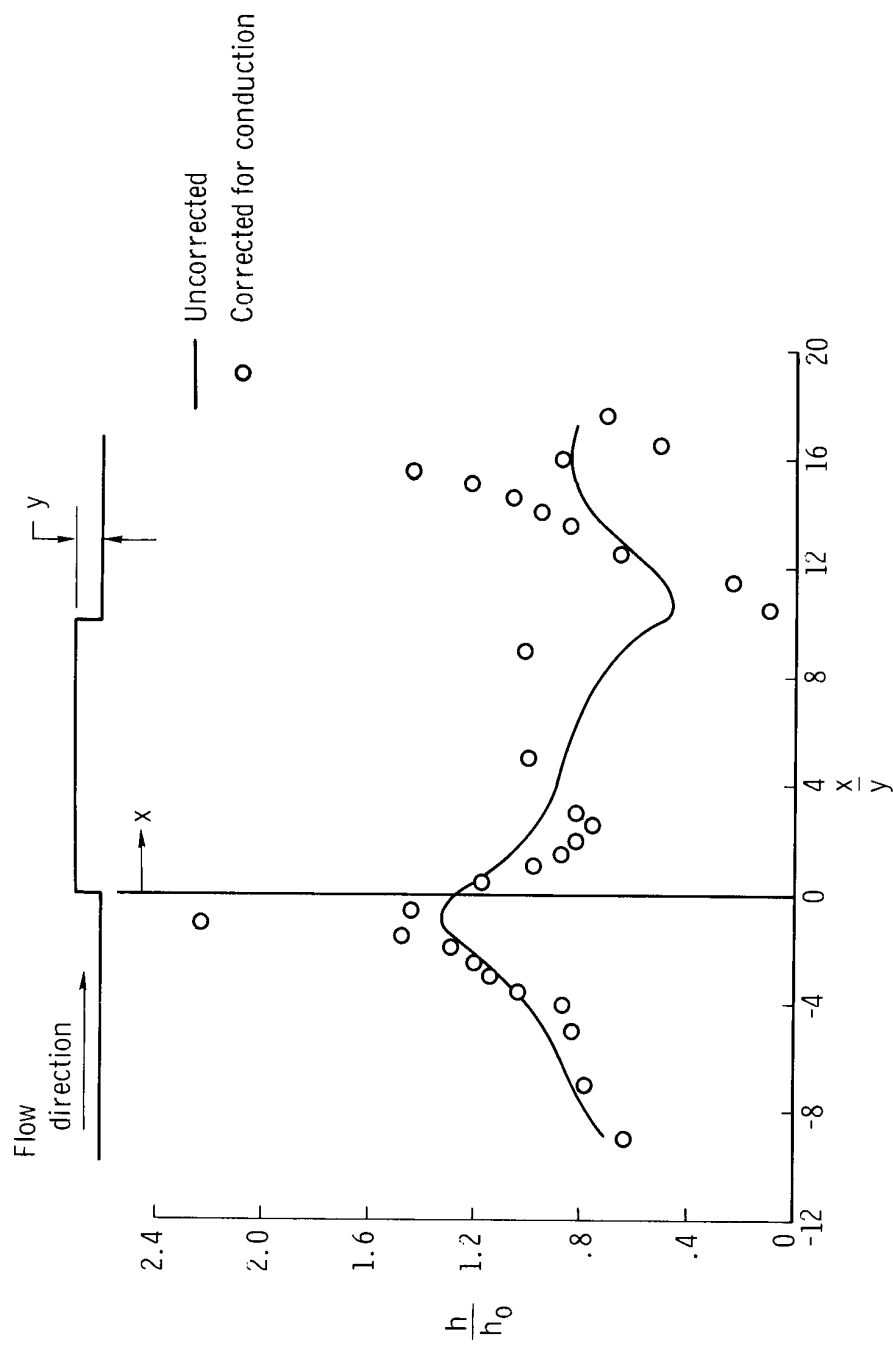


Figure 8. — Temperature distribution along the step configuration at data time 2.8 seconds.





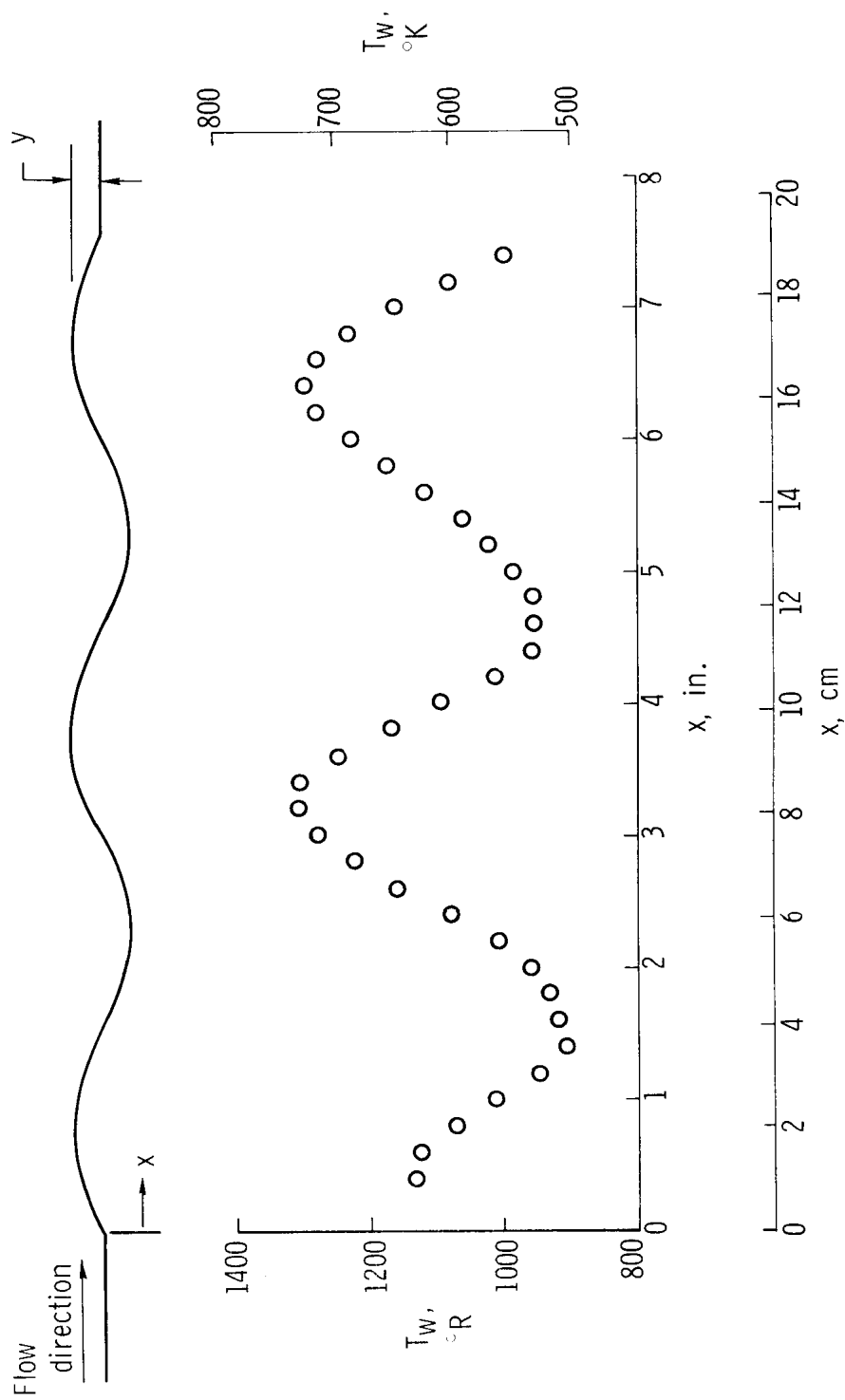


Figure 10.— Temperature distribution over the wave configuration at data time 2.8 seconds.

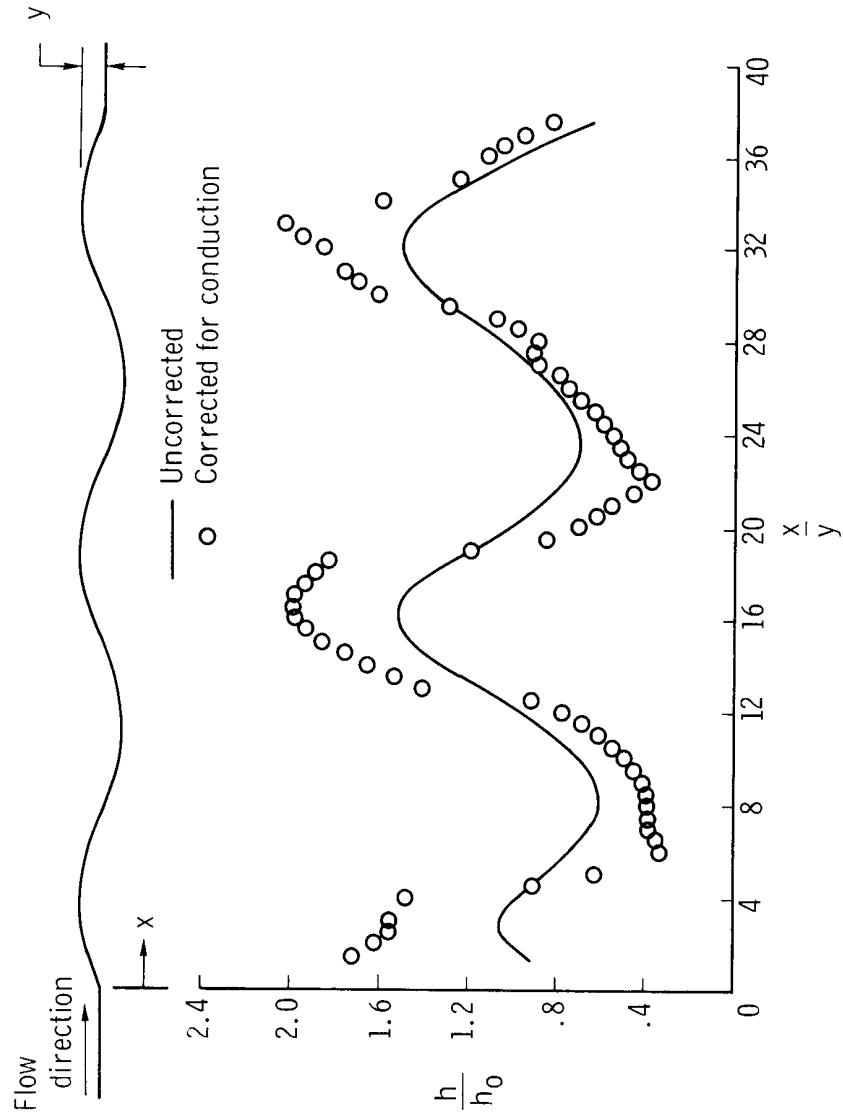


Figure 11. - Heat-transfer ratio distribution across the wave configuration.

$$h_0 = 1.64 \times 10^{-3} \frac{\text{Btu}}{\text{ft}^2 \cdot \text{sec} \cdot ^\circ \text{R}} \left( 33.5 \frac{\text{J}}{\text{m}^2 \cdot \text{sec} \cdot ^\circ \text{K}} \right).$$

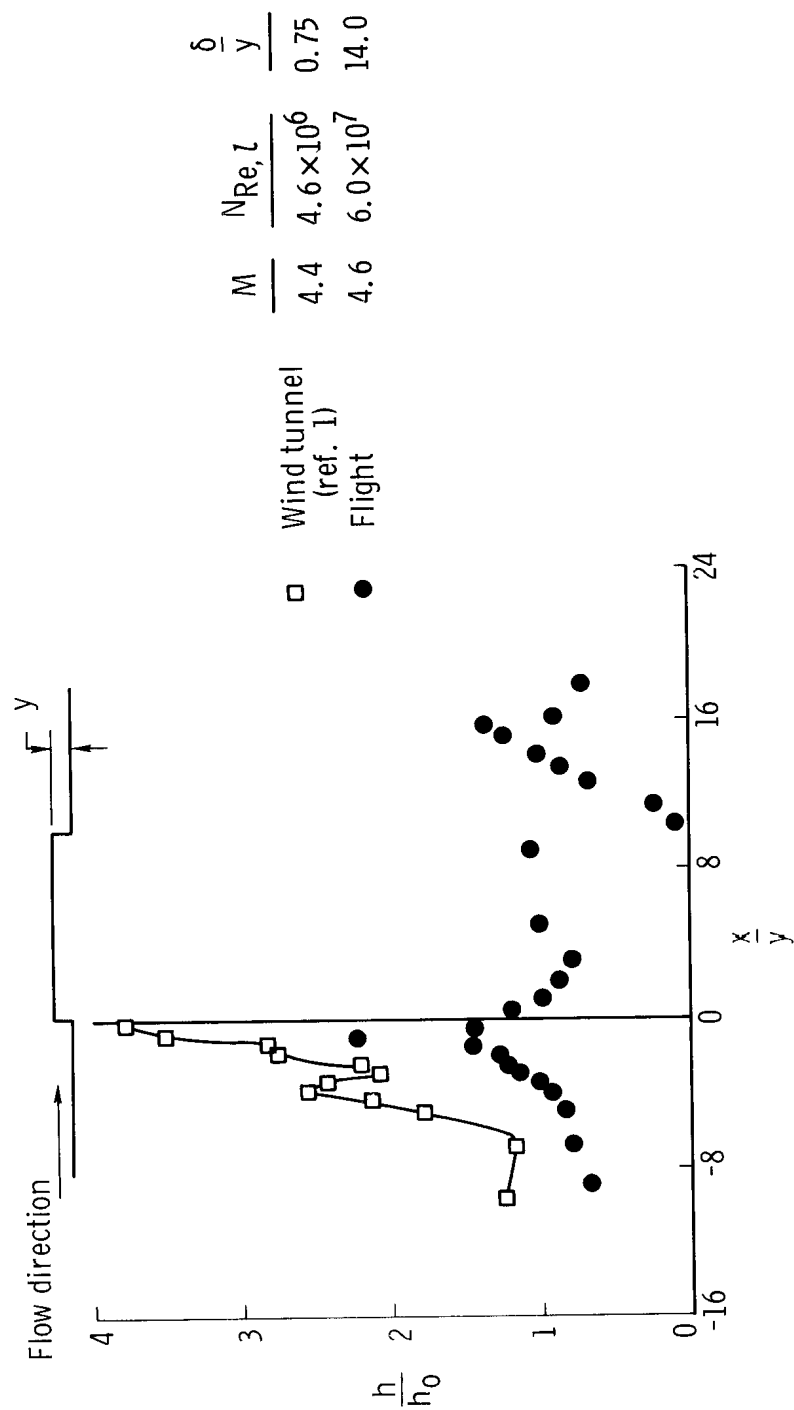


Figure 12. - Comparison of heat-transfer data from flight and wind-tunnel for a forward-facing step.

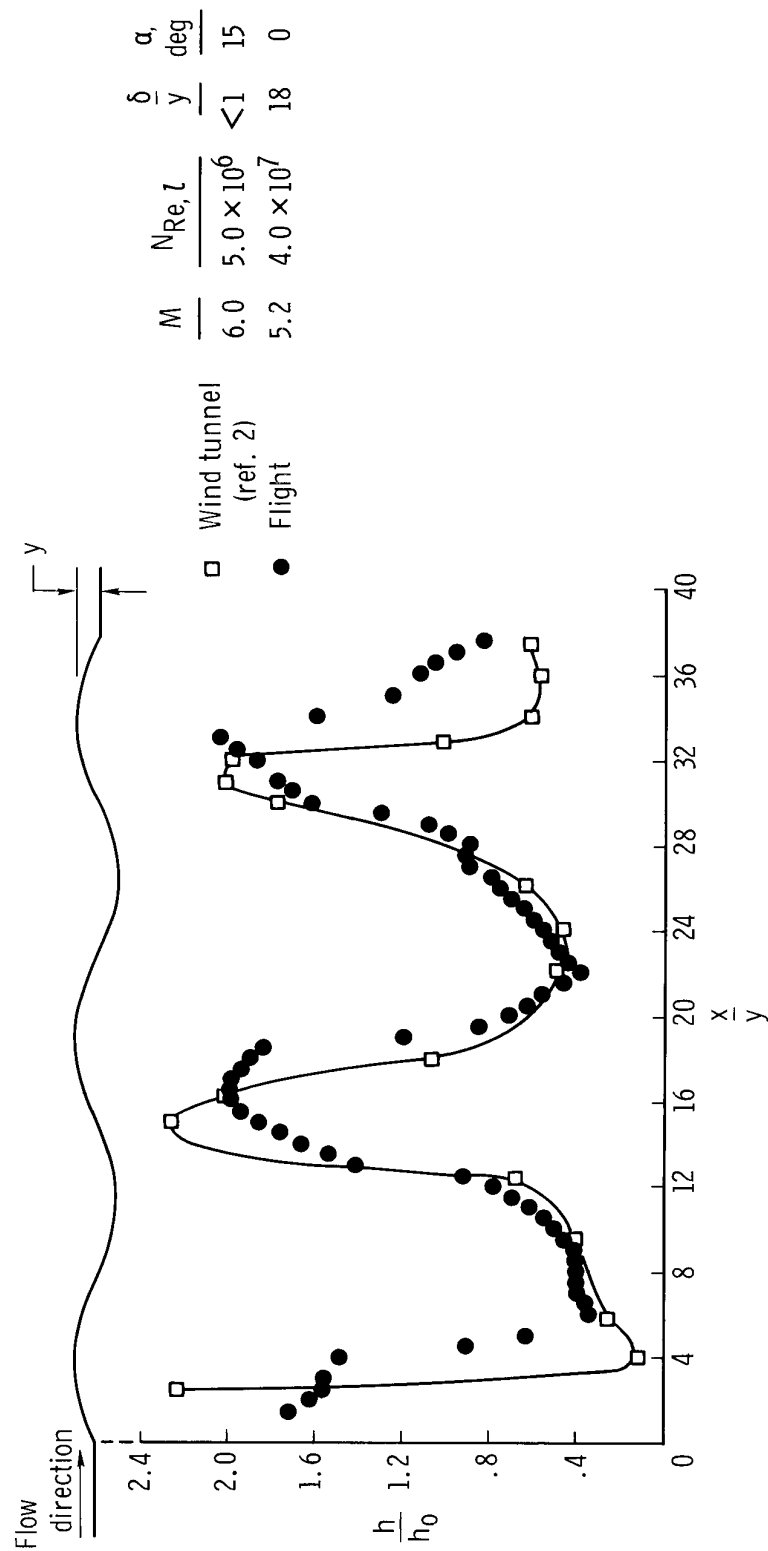


Figure 13.— Comparison of heat-transfer data from flight and wind tunnel for a wave train.